

Role of the reaction product in the solidification of Ag–Cu–Ti filler for brazing diamond

T. YAMAZAKI^a, A. SUZUMURA^b

Faculty of Engineering, Tokyo Institute of Technology, 2-12-1 O-okayama Meguro-ku Tokyo 152, Japan

E-mail: ^ayamazaki@postman.riken.go.jp; ^bsuzumura@mep.titech.ac.jp

In order to reveal the mechanism for brazing diamond using Ag–Cu–Ti filler metal, thermoanalysis of elemental metals (silver and copper) either with added diamond micropowder or with added titanium carbide micropowder as nucleant were investigated to detect undercoolings. No undercooling for the solidification of silver with added titanium carbide powder was detected by the thermoanalytical curve, and also no undercooling for copper with added diamond powder was detected. These phenomena suggest that titanium carbide powder acts in the solidification of silver effectively as a nucleant and that diamond powder also acts in the solidification of copper as a nucleant. Fine-grained silver was observed in the micrograph of the silver added with titanium carbide powder. The results of the calculations on the planar disregistry, δ , and the dispersion energy, E_{disp} revealed that the Ag (100)–TiC(100) interface and Cu(100)–diamond (100) interface are more stable than the other combinations. The results of undercoolings of various specimens correlated with both planar disregistry and dispersion energy. According to these results, the titanium carbide reaction product is considered to play an important role in the solidification of silver. The brazing strength is considered to arise from the solidification of the brazing filler metal from the titanium carbide reaction product. © 1998 Chapman & Hall

1. Introduction

In our previous investigation, a unidirectional solidification method for brazing diamond was carried out. This method is explained next.

The brazing specimen was composed of one diamond, a sheet of brazing filler metal and a base thin metal plate. The diamond was mounted on the metal plate. The brazing filler metal was put between the diamond and the metal plate. The brazing specimen was cooled from the top of the diamond by contact with a copper cooling mass; as a result, the brazing filler metal was solidified from diamond surfaces.

In the case of the $6 \times 10^6 \text{ W m}^{-2}$ cooling rate, the solidified structure of brazing filler metal from diamond showed dendrite arms of silver in which about 14 at % Cu was detected. Growth of copper crystals from diamond was scarcely observed there.

The shear strength of diamond (100) specimens brazed by this method was about twice that made by the usual furnace brazing [1, 2]. It was more than 130 MPa, which implies that, for brazing diamond, the solidification of the brazing filler metal is important.

In order to investigate the solidification mechanism of brazing filler metal from diamond, the thermoanalyses and the solidified structures of elemental metals either with added diamond micropowder or with added titanium carbide micropowder were investigated.

From the viewpoint of the relationships between the lattice mismatch and the interfacial energy, the role of the titanium carbide reaction product in the brazing diamond process is considered.

2. Experimental procedure

About 15 g of copper flakes which had a high purity (99.99%) were measured out. Diamond powder (35 μm in diameter) as nucleant was measured out at the rate of about 0.04% of the mass of copper flakes and laid on the bottom of the quartz crucible. A Pt–(Pt–13 wt % Rh) thermocouple was embedded in the bottom of a small quartz crucible as shown in Fig. 1 and located about 5 mm above the bottom of the large crucible. The small quartz crucible was used in order to protect the thermocouple and to prevent heterogeneous nucleation at the thermocouple surface. The copper flakes were poured into it so as not to move the thermocouple. Titanium carbide polycrystal powder (5 μm in diameter) of the same mass as that of the diamond powder was measured out into the bottom of another quartz crucible. The thermocouple and copper flakes were settled as mentioned above. No nucleant was poured into the other crucible for comparison with those with added nucleant.

About 10 g of silver balls which had a high purity (99.999%) were measured out. A Pt–(Pt–13 wt % Rh) thermocouple was located at the same position as for

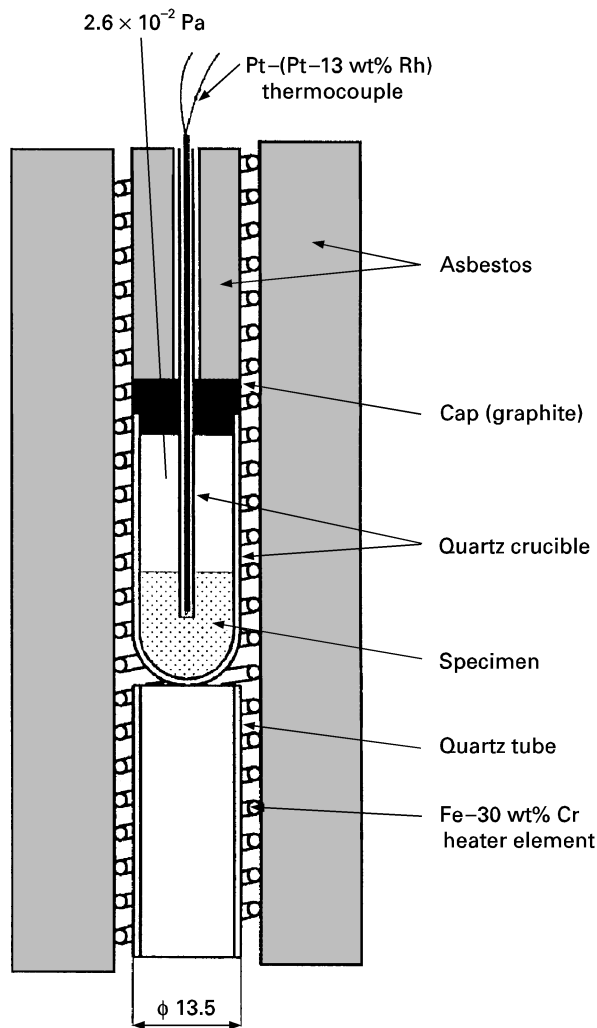


Figure 1 Thermoanalytical equipment.

the copper specimens. Diamond powder was measured out at the rate of about 0.04% of the mass of the silver balls and laid on the bottom of the quartz crucible. The crucible into which the silver balls were

poured was prepared in the same way as for the copper specimens. Titanium carbide powder of the same mass as that of the diamond powder was measured out into the bottom of another quartz crucible. The thermocouple and silver balls were settled as mentioned above. No nucleant was poured into the other crucible for comparison with those with added nucleant.

The furnace shown in Fig. 1 was evacuated by a rotary pump and an oil diffusion pump. It was operated at 2.6×10^{-2} Pa or less. The temperature of the specimen was raised slowly, and after the metal had melted entirely, it was maintained for 600 s and cooled slowly. The cooling rate was 0.1 K s^{-1} .

The thermoanalytical curves of a series of various specimens were measured with the Pt-(Pt-13 wt% Rh) thermocouple, which has good linearity at high temperatures such as the melting points of copper and of silver. The thermocouple voltage was amplified tenfold, since this thermocouple has a small thermoelectromotive force, and was recorded with an X-Y recorder in the range of 20 mV. The amplifier has a 0.05% linearity error. The X-Y recorder has a 0.25% accuracy error. Undercoolings were detected from these analytic curves. The solidified morphologies of each specimen were observed by microscopy after etching.

3. Results

The main examples of thermoanalytical curves for various specimens are shown in Fig. 2. Fig. 2a is a thermoanalytical curve for a pure copper specimen with no nucleant added, Fig. 2b is for a copper specimen with added diamond powder, Fig. 2c is for a copper specimen with added titanium carbide powder, Fig. 2d is for a silver specimen with no nucleant added and Fig. 2e is for a silver specimen with added titanium carbide powder.

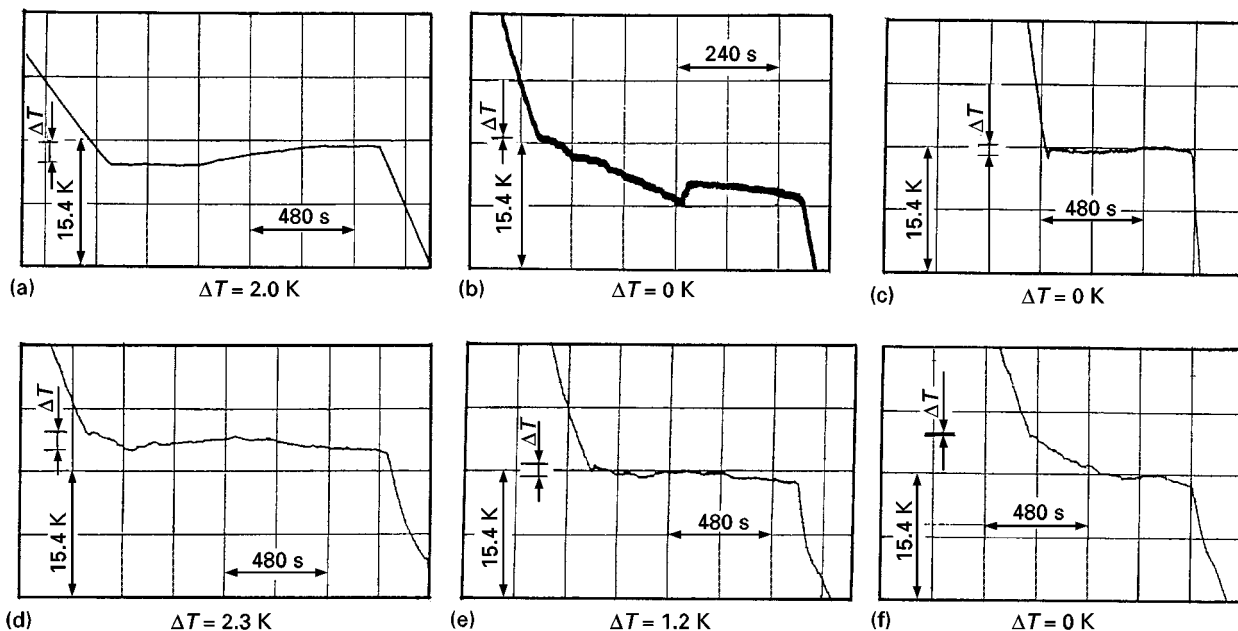


Figure 2 Thermoanalytical curves for (a) pure copper, (b) copper with added diamond, (c) copper with added titanium carbide, (d) pure silver, (e) silver with added diamond and (f) silver with added titanium carbide.

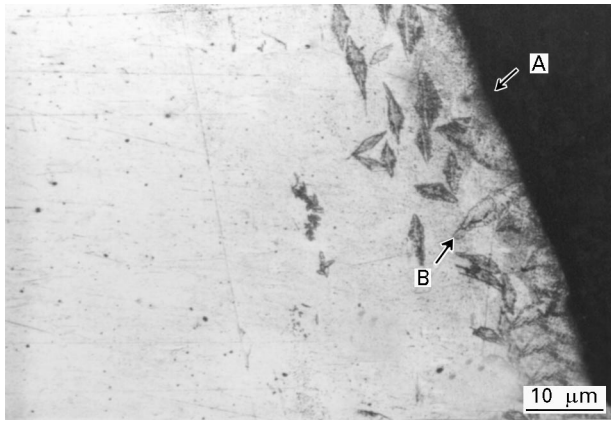


Figure 3 Solidified structure of pure silver.

The undercooling for pure copper with no nucleant added is 2.0 K, and the thermoanalytical curve shown in Fig. 2a shows clear supercooling. No undercooling for the copper specimen with added diamond powder is detected in Fig. 2b. This was confirmed from the emission of heat of solidification at the copper melting point. The undercooling for the copper specimen with added titanium carbide powder is 1.5 K. The thermoanalytical curve shown in Fig. 2c shows clear supercooling.

The slope of the thermoanalytical curve in Fig. 2d for pure silver changes at the melting point of silver owing to a little crystallization from the quartz crucible. This was confirmed by the micrograph shown in Fig. 3. The quartz crucible wall which protects the thermocouple is labelled A in Fig. 3. The silver crystals B grow from the wall of the small quartz crucible. This undercooling was 2.3 K. The undercooling for the silver specimen with added diamond powder was 1.0 K according to Fig. 2e. It is similar to Fig. 2d. No undercooling for the silver specimen with added titanium carbide powder is detected in Fig. 2f, similar to Fig. 2b.

Table I shows the results of undercooling, ΔT , for no nucleant, diamond powder nucleant and titanium carbide powder nucleant. The addition of diamond powder influences the solidification of copper; so the undercooling, ΔT , is 0.0 K. On the other hand, the

TABLE I Values of undercooling ΔT for the various additives; no nucleant, diamond powder nucleant and titanium carbide powder nucleant

Base metal	ΔT (K)		
	No nucleant	Diamond nucleant	TiC nucleant
Cu	1.8 ± 0.2	0.0	1.5 ± 0.3
Ag	2.3	1.2 ± 0.2	0.0

addition of titanium carbide powder has little influence on the solidification; so undercooling was almost same value as the specimen without a nucleant. For the solidification of silver, the addition of titanium carbide powder also has an effect; so the undercooling was 0.0 K. On the other hand, the addition of diamond powder has little effect on the solidification of silver; so the undercooling was 1.2 ± 0.2 K. This value should be compared with that of the specimen without a nucleant whose undercooling was 2.3 K.

Micrographs of the solidified structures of the silver specimens are shown in Fig. 4. Fig. 4a shows the solidified structure of silver with added diamond powder. The 30 μm diamond particles A is excluded from the silver grain B, because this silver crystal grain grows from the left-hand side of the figure. This indicates that diamond powder has little influence on the silver crystallization. In contrast, the solidified structure of silver with added titanium carbide powder is shown in Fig. 4b, where approximately 50 μm silver crystal grains are observed on the left-hand side. One approximately 5 μm titanium carbide particle A is in the silver grain B. This indicates that heterogeneous nucleation has occurred.

Micrographs of copper solidified structures are shown in Fig. 5. One approximately 20 μm diamond particle A is in the grain of copper and is not expelled to the grain boundaries as shown in Fig. 5a. In contrast with this, 5 μm titanium carbide powder is excluded from the copper grain and forms a grain boundary A as shown in Fig. 5b. Titanium carbide powder has little influence on the crystallization of copper.

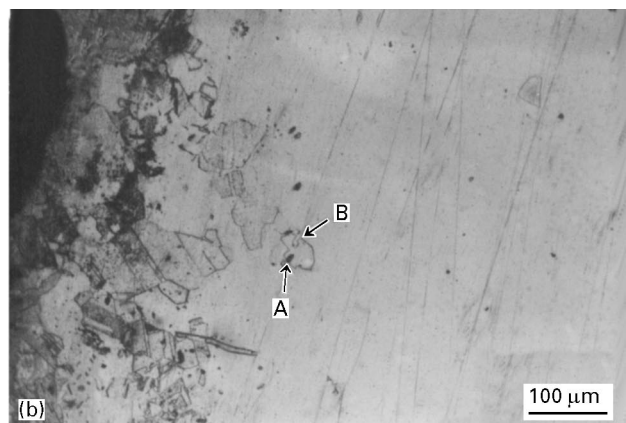
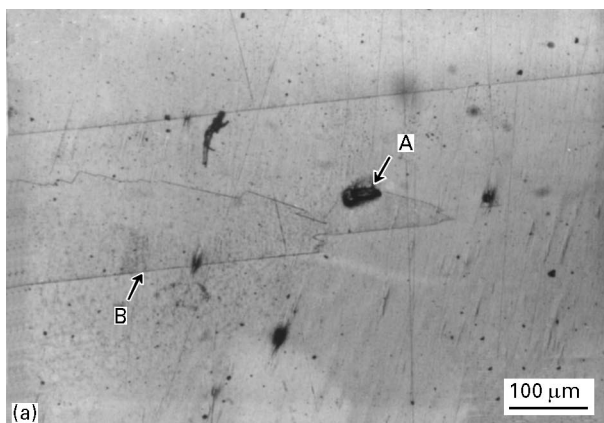


Figure 4 Solidified structures of (a) silver with added diamond powder and (b) silver with added titanium carbide powder.

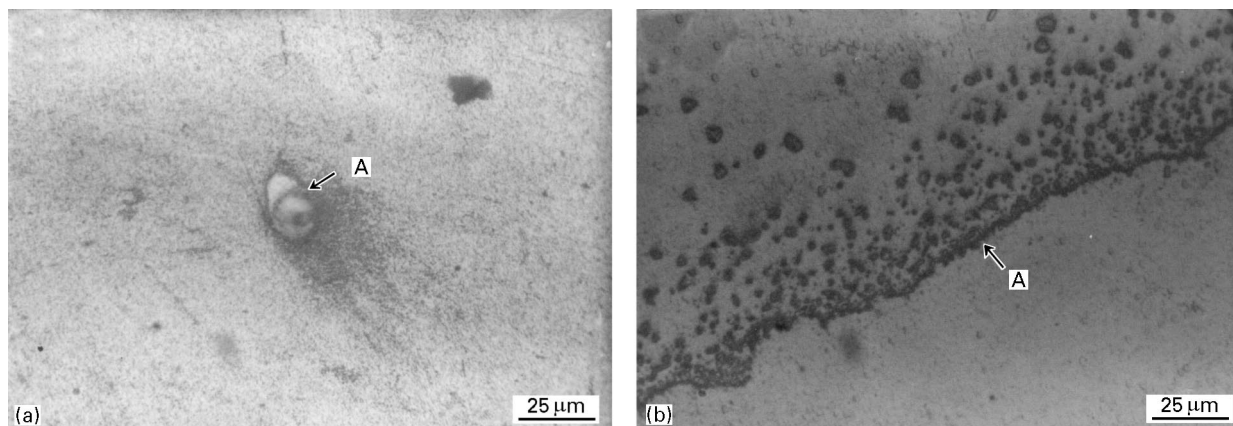


Figure 5 Solidified structures of (a) copper with added diamond powder and (b) copper with added titanium carbide powder.

4. Discussion

4.1. Introduction of lattice mismatch parameter

A parameter of lattice mismatch between nucleant and metal is introduced to discuss the solidification of elemental metals of the brazing filler metal. The parameter is called the planar disregistry as advocated by Bramfitt [3]. Planar disregistry, δ (%), is expressed in the following equation, taking account of the lattice mismatches on the low-index planes and the gap in three directions:

$$\delta = \frac{1}{3} \sum_{i=1}^3 \frac{|d[uvw]_c^i \cos \theta - d[uvw]_s^i|}{d[uvw]_s^i} \times 100 \quad (1)$$

where $d[uvw]_c$ is the nearest-neighbour distance on the low-index plane of the nucleant, $d[uvw]_s$ is the nearest-neighbour distance on the low-index plane of the solid crystal (metal) and θ is the angle between the close-packed directions of the two substances.

Fig. 6a and b shows the stable sites of diamond (100) and titanium carbide (100), respectively. Taking into account the dangling bond on the diamond surface shown in Fig. 6a, the stable sites and the interatomic distances were determined. Two dangling bonds shown as small ellipses from two carbon atoms point to one stable site. The stable sites of the unit lattice are shown as a square drawn with broken lines. The shaded circles are the second-layer carbon atoms. The distances on the stable sites are calculated from the lattice constant of diamond which has covalent bonds. In the case of titanium carbide (100), the stable sites of the unit lattice are shown in Fig. 6b. These sites are situated on carbon atoms and not on titanium atoms as shown by calculations for the dispersion energy mentioned in the next section.

For the elemental metals, the interatomic distances are obtained from the lattice constant on the lattice plane which fitted the stable sites of the diamond and titanium carbide nucleants, respectively.

4.2. Method of calculation of the interfacial energy related to the lattice mismatch parameter

Silver and copper elements are inert to carbon. They do not form stable carbides [4]. It is assumed that the

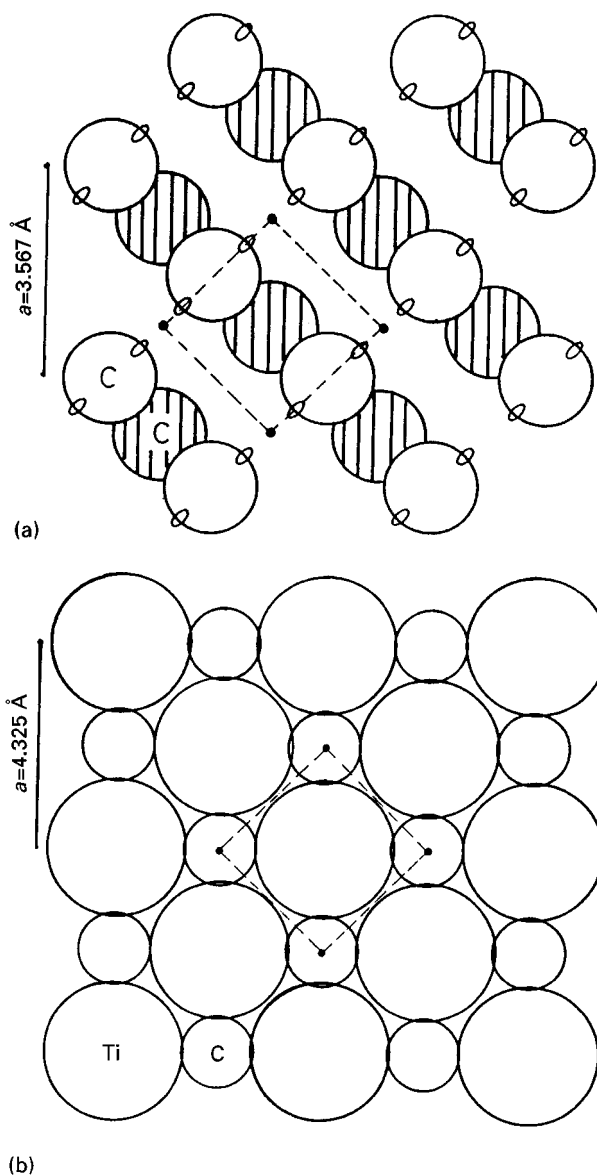


Figure 6 Stable sites on (a) diamond (100) and (b) titanium carbide.

interactions between the nucleant and metal are not of a chemical nature, so that the physical interactions are decisive for these systems.

With the help of the expression for the dispersion force potential, it is possible to estimate quantitatively

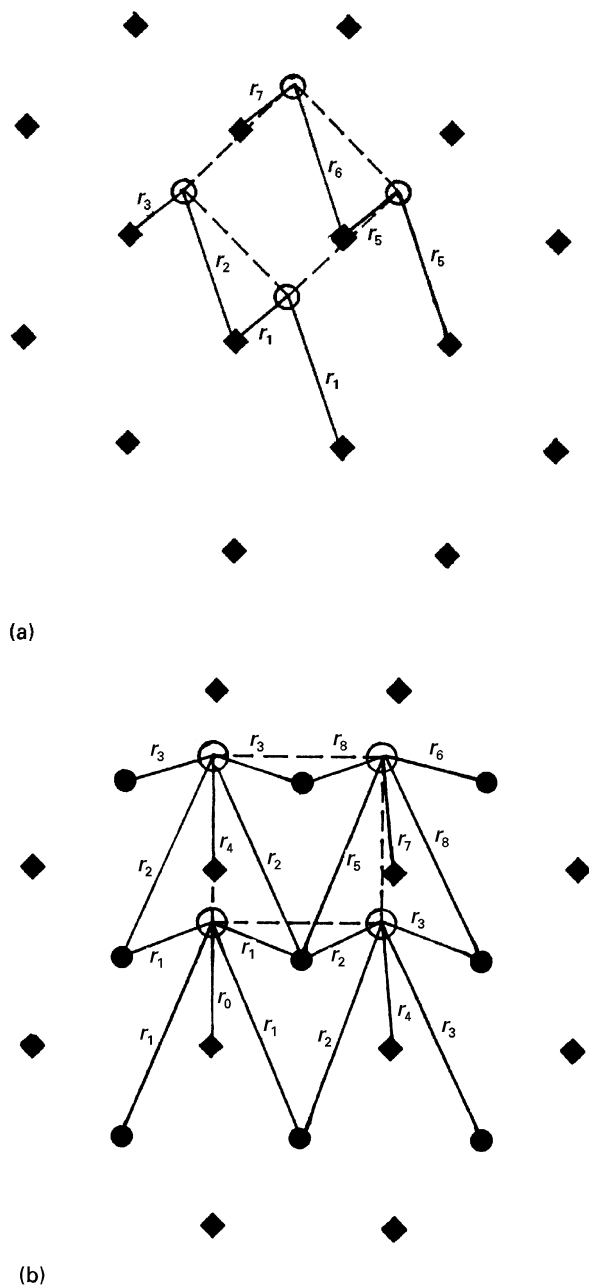


Figure 7 Interatomic distances of (a) copper–diamond ((○), Cu; (■), C) and (b) silver–titanium carbide ((○), Ag; (●), Ti; (■), C) in order to calculate the dispersion energy.

the interfacial energy, E_{disp} , between the nucleant and metal atoms in contrast with planar disregistry. One can use the expression for the interaction between a pair of atoms:

$$E_{\text{disp}} = \frac{3}{2} \frac{\alpha_1 \alpha_2}{R^6} \frac{I_1 I_2}{I_1 + I_2} \quad (2)$$

where α_1 and α_2 are the polarizabilities, I_1 and I_2 are the first ionization potentials of atom 1 and 2, respectively, and R is the distance between them. The polarizability was approximately determined from

$$\alpha \approx \frac{e^2 h^2}{4\pi^2 m I^2} \quad (3)$$

where h is the Planck constant, m is the electron mass and I is the first ionization potential.

More assumptions have to be made in order to relate this to the planar disregistry. Fig. 7 gives us an

idea of how to calculate the interatomic distances. Each crystal plane of the nucleant and metal is atomically smooth. In the case in Fig. 7a which shows diamond (100), four metal atoms which have the bulk lattice constant and lattice plane, are near carbon atoms but are parallel to diamond (100); one atom of the metal is in contact with the carbon atoms. The interatomic distances are determined in this situation. r_i are the distances between the carbon atom and the metal atom calculated geometrically. The dispersion energy of two carbon atoms per metal atom is calculated from Equation 2, and these are summed for four metal atoms.

In the case in Fig. 7b which shows titanium carbide (100), the dispersion energy of one metal atom is calculated from the distance between four titanium atoms of titanium carbide and the metal atom, and between the five carbon atoms of titanium carbide and the metal atom. These r_i are the distances in Equation 2. The distances between each pair of four carbon atoms and one metal atom are not shown in Fig. 7b, because the figure would become too complicated. These dispersion energies are summed for four metal atoms to give E_{disp} per four atoms.

4.3. Relation between undercooling, planar disregistry and dispersion energy

The values of undercooling are presented in Table I, for no nucleant, diamond micropowder nucleant and titanium carbide micropowder nucleant. The results of the calculation on planar disregistry δ are presented in Table II. These values are the lowest of the combinations of each crystal lattice plane of both substances. The values for the dispersion energy E_{disp} for four metal atoms are presented in Table III.

Planar disregistry is a parameter which indicates an effective additive for fine-grained metal. It is expected that this parameter will be able to predict whether heterogeneous nucleation will occur or not for the stable sites of diamond and titanium carbide. From the comparison between Table I and Table II, the copper–diamond and silver–titanium pairs for which undercoolings were not detected have low planar disregistries. From the comparison between Table I and Table III, these pairs have high values of dispersion energy.

According to the results of high-shear-strength specimens brazed by the unidirectional solidification method, the strength was influenced by the solidification phenomenon. It is necessary for heterogeneous nucleation to occur at the brazing interface between diamond and brazing filler metal. Planar disregistry and dispersion energy are considered to be useful. In the case of the solidification of elemental metals from diamond, the values of planar disregistry and dispersion energy are compared with each other. The value of planar disregistry for Cu(100)–diamond (100) is 1.327%. In contrast with this, the value for Ag(100)–diamond (100) is 12.71%. According to this comparison, the interfacial orientation of Cu(100)–diamond (100) is more suitable than that of

TABLE II Values of planar disregistry for copper (100)–diamond (100), copper (100)–titanium carbide (100), silver (100)–diamond (100) and silver (100)–titanium carbide (100) interfaces

Base metal	Interface	δ
Cu	Cu (100)–diamond (100)	1.327
Cu	Cu (100)–TiC(100)	19.52
Ag	Ag(100)–diamond (100)	12.71
Ag	Ag(100)–TiC(100)	5.728

TABLE III Interfacial energy E_{disp} (10^{-19} J for few atoms) related to planar disregistry

Base metal	E_{disp} for few atoms for the following nucleants	
	Diamond	TiC
Cu	1.53	1.11
Ag	0.771	1.40

Ag(100)–diamond (100). This suggests that it is easier for the solidification of copper to occur from diamond (100) than for the solidification of silver to occur.

In the case of the titanium carbide reaction product, the value of planar disregistry for Cu(100)–TiC(100) is 19.52%. In contrast, the value for Ag(100)–TiC(100) is 5.728%. According to this comparison, the interfacial orientation of Ag(100)–TiC(100) is more suitable than that of Cu(100)–TiC(100). This suggests that it is easier for the solidification of silver to occur from titanium carbide powder than for the solidification of copper to occur.

The dispersion energy is related to the planar disregistry as presented in Table III. The dispersion energy for the Cu(100)–diamond (100) interface is -1.53×10^{-19} J for four atoms. In contrast, the value for the Ag(100)–diamond (100) interface is -7.71×10^{-20} J for four atoms. According to this comparison, the formation of the interface between copper and diamond is more preferable than that between silver and diamond.

The dispersion energy for the Cu(100)–TiC(100) interface is -1.11×10^{-19} J for four atoms. In contrast, the value for the Ag(100)–TiC(100) interface is -1.40×10^{-19} J for four atoms. The formation of the interface between silver and titanium carbide is more preferable than that between copper and titanium carbide.

Heterogeneous nucleation is better than homogeneous nucleation and pore nucleation of the brazing

filler metal at the brazing interface. The elemental metals of brazing filler metal need to have a low planar disregistry with diamond and titanium carbide. The titanium carbide reaction product plays an important role in the solidification of silver; the stable interface between diamond and the brazing filler metal is formed by this phenomenon.

5. Conclusions

The results of undercoolings of silver and copper including additives, namely diamond powder and titanium carbide powder are correlated with the solidification behaviour of each specimen. When no undercoolings were detected by thermal analyses on specimens, this meant that these additives act in the solidification of metals as an effective nucleant. One example is given in the micrograph of fine-grained silver with added titanium carbide powder.

The results of the calculations on planar disregistry, δ , and dispersion energy, E_{disp} , reveal that the Ag(100)–TiC(100) interface and the Cu(100)–diamond (100) interface are more stable than the other combinations. According to these results, heterogeneous nucleation is better than homogeneous nucleation and pore nucleation of elemental metals of the brazing filler metal. The elemental metals need to have a low planar disregistry with diamond and the reaction product surface.

Acknowledgements

The authors wish to thank the Tokyo Diamond Co Ltd for the supply of diamonds, and to express their indebtedness to Mr S. Okano, Tokyo Institute of Technology, who made a substantial contribution to the experimental programmes.

References

1. T. YAMAZAKI and A. SUZUMURA, in Proceedings of the Sixth International Symposium of the Japan Welding Society, Vol. 1 (Japan Welding Society, Tokyo, 1996) p. 125.
2. A. SUZUMURA, T. YAMAZAKI, K. TAKAHASHI and T. ONZAWA, *Quart. J. Jpn Welding Soc.* **12** (1994) 509 (in Japanese).
3. B. L. BRAMFITT, *Mater. Trans.* **1** (1970) 1987.
4. JU. V. NAIDICH, *Prog. Surf. Membrane Sci.* **14** (1981) 409.

Received 23 February 1996
and accepted 25 September 1997